NAL TR-188T

UDC 531.38:
681.08:
629.7.062.2

TECHNICAL REPORT OF NATIONAL AEROSPACE LABORATORY

TR-188T

Analysis of the Anisoelastic Errors of a Floated Single Degree of Freedom Integrating Gyro

Masao OTSUKI, Hirokimi SHINGU, Jyoji TABATA,
Takao SUZUKI and Shigeharu ENKYO

June 1973

NATIONAL AEROSPACE LABORATORY

CHŌFU, TOKYO, JAPAN

List of NAL Technical Reports

TR-166 Fundamental Analyses of Gimbal-Engine Positioning Hydraulic Control System Made Use of DPF Servovalve	Shigeki HATAYAMA & Hajime KOSHISHI	Nov. 1968
TR-167 Measurements of Heat Transfer Reduction by Ablation at Stagnation Region	Shigeaki NOMURA	Nov. 1968
TR-168 On the Orbit Determination Procedures for the Doppler Frequency Measurement with Angular Measurement Tracking System	Ryozo TORIUMI, Kazuo MATSUMOTO, Kazuo HIGUCHI, Hayato TOGAWA & Takeo KIMURA	Nov. 1968
TR-169 Design and Construction of VTOL Flight Simulator System	Kazuo HIGUCHI, Moriyuki MOMONA, Noriko MIYOSHI, Masanori OKABE, Rokuro YAMAMOTO & Hiroyasu KAWAHARA	Dec. 1968
TR-170 System Studies on Automatic Longitudinal Stabilization Control Systems for STOL Aircraft Part 1 Automatic Attitude Systems	Yuso HORIKAWA & Mikihiko MORI	Dec. 1968
TR-171T Simple Flow Characteristics Across a Strong Shock Wave	Kenneth K. YOSHIKAWA	Feb. 1969
TR-172 Measurement of Dynamic Stability Derivatives of Cones and Delta-Wings at High Speed	Mitsunori YANAGIZAWA	Feb. 1969
TR-173T The Coupling Effect of Radiative Heat on Convective Heat Transfer	Kenneth K. YOSHIKAWA	Feb. 1969
TR-174 Difference Method for Navier-Stokes Equation	Hajime MIYOSHI	Apr. 1969
TR-175 Stalling Characteristics of the NACA 0012 Aerofoil Section at Low Reynolds Numbers	Yasuharu NAKAMURA, Koji ISOGAI & Hiroshi EJIRI	Jun. 1969
TR-176 On the Vibration of Axial-flow Turbomachine Blades (I) Natural Frequency, Mode and Vibratory Stress Distribution	Toshio MIYACHI, Shoji HOSHIYA, Yasuyuki SOFUE, Saburo AMIHOSHI, Tadasuke IWABU & Katsumi TAKEDA	Jul. 1969
TR-177 Thrust Magnitude Control of Solid Rocket Motors —Characteristics Analysis and Small Motor Tests—	Tomifumi GODAI, Yoshinori YUZAWA, Katsuya ITO & Hisao NISHIMURA	Jul. 1969
TR-178 Necessary Conditions for the Optimal Weighting Matrices of Quadratic Performance Index to Maximize the Measure of the Controllable Set	Nagakatsu KAWAHATA	Jul. 1969
TR-179 Measurements of Transient Ablation of Teflon	Shigeaki NOMURA	Aug. 1969
TR-180 Measurement and Analysis of Atmospheric Turbulence over the SUZUKA Mountain Range	Kazuyuki TAKEUCHI, Koichi ONO, Kosaburo YAMANE, Toichi OKA & Tokuo SOTOZAKI	Aug. 1969
TR-181 Unsteady Surface Pressure on an Oscillating Aerofoil at High Mean Angles of Attack with Special Reference to Stall Flutter	Yasuharu NAKAMURA, Koji ISOGAI & Hiroshi EJIRI	Aug. 1969
TR-182 On the Natural Viblation of Plates Restrained at Several Points	Taketoshi HANAWA, Yasuo TADA, Hideo IZUMI & Shinichi KOSHIDE	Sep. 1969

Analysis of the Anisoelastic Errors of a Floated Single Degree of Freedom Integrating Gyro*

By Masao OTSUKI**, Hirokimi SHINGU**, Jyoji TABATA***,
Takao SUZUKI** and Shigeharu ENKYO**

浮動型1自由度積分ジャイロに加速度を作用させたときに発生する誤差をジンバルの弾性モデルによって理論的に解析し，実験結果と比較・検討した結果，その誤差は定常加速度に関しては加速度の自乗に比例する特性を有することが，振動加速度に関してはジャイロの入力軸，スピン軸方向の剛性の相違（不等弾性）による固有共振周波数の差のために，ある周波数領域(1000～2000 Hz) で異常に大きな値を有することがそれぞれ解明された。

理論式の誘導，シミュレーション，タンブリングテスト，振動実験の結果からジャイロの誤差要因を分析し，かつジャイロの誤差評価を行なった。これにより定常，振動加速度による誤差は共にジャイロロータのベアリングを含むジンバル系の不等弾性に起因することが理論的，実験的に結論づけられた。

SUMMARY

A floated single-degree-of-freedom integrating (SDF) gyro is used to sense angular rates of vehicle motion, but senses the errors called "drift rates" by applying the acceleration whose direction is perpendicular to its output axis. The drift rate, which is proportional to the square of acceleration magnitude, is caused by a difference in compliance of the gimbal between the input axis and the output axis, and is called "anisoelastic error".

In this paper, the anisoelastic error was analyzed theoretically and experimentally through derivation of the theoretical formula, tumbling test, vibration experiment and simulation. When vibrational accelerations were applied to the gyro, the anisoelastic error grew remarkably over a certain frequency range because of a difference in natural resonant frequency depending on the anisoelasticity, and was the same as that caused by steady acceleration at the frequency without the influence of natural resonance. The experimental results of the anisoelastic error were closely proportional to the square of acceleration magnitude and their frequency characteristics showed a tendency similar to the simulations.

1. PREFACE

When the acceleration is applied to a single-degree-of freedom gyro, the acceleration causes a slight elastic deformation on the gimlal system containing spin rotor bearings, the center of gravity of the float deflects from the center of buoyancy, and so the error called "drift rate" occurs. The direction of the deflection of the center of gravity has a component perpendicular to the applied acceleration for the nonuniformity of the gimbal rigidity, and a torque is generated. The component along the gyro output axis of this torque causes the drift rate, which is proportional to the product of the square of the acceleration magnitude and the difference between the compliance of gimbal structure along the input axis and the one along the output axis. This drift rate is called "anisoelastic error". So far, in the case of treating this kind of error the effect of steady accelerations has mainly been considered. However it is necessary to study theoretically and experimentally the drift rate caused by vibrational acceleration in order to develop the preciser gyro under the vibration environment which is given by the motion of a space vehicle.

In this paper at first the theoretical formula on the drift rate, which presents the steady acceleration term and the vibrational acceleration term, is derived from the elastic model of the gimbal showing the deflection of the center of gravity of the float due to the elastic deformation of the gimbal system containing spin rotor bearings when steady and vibrational accelerations act on the gyro in different directions at the same time. After that, experimental results

* Received March 4, 1972.

** Instrumentation and Control Division.

*** Formerly instrumentation and Control Division, present National Space Development Agency of Japan (NASDA)

of drift rates caused by steady and vibrational accelerations from tumbling test and vibration experiment are shown.

From the results of above-mentioned, theoretical and experimental investigations, it is clarified that the drift rates vary depending on the magnitude, direction and frequency of acceleration in the case of the gyro with anisoelasticity of the gimbal system containing spin bearings.

2. NOMENCLATURE

C: Viscous damping coefficient between the gyro float and the gyro case.

c_{x2}, c_{z2}: Damping coefficients along x_2 and z_2 axes in the elastic deformation of gimbal.

f: Frequency of vibrational acceleration (Hz)

$F_{x1}, F_{z1}, F_{x2}, F_{z2}$: Components along x_1, z_1, x_2 and z_2 axes of the forces which act on the center of gravity of the float.

g: Gravitational acceleration (980 cm/sec^2)

G: Center of gravity of the float

H: Angular momentum of the rotor about its spin axis (9.931×10^4 gr.cm^2/sec)

J: Moment of inertia of the float about its output axis.

K: Elastic restraint constant.

M: Float mass (75.9 gr)

O: Origin of the coordinate (Center of buoyancy of the float)

$0\text{-}x_a y_a z_a$: Case-fixed coordinate system

$0\text{-}x_1 y_1 z_1$: Gimbal-fixed coordinate system

$0x_1, 0y_1, 0z_1$: Input axis, Output axis, Spin axis

$0x_2, 0z_2$: Axes of compliance

T_{Dy1}: Disturbance torque which acts on the float about output axis

$x_{1G}, y_{1G}, z_{1G}, x_{2G}, y_{2G}, z_{2G}$: x_1, y_1, z_1, x_2, y_2 and z_2 components of the deflection of the center of gravity in non-accelerated state.

α_0, α: Magnitude of steady and vibrational accelerations

β: Difference angle of $0x_2, 0z_2$ directions from $0x_1, 0z_1$ directions

γ: Gyro output angle

$\delta_{x1}, \delta_{z1}, \delta_{x2}, \delta_{z2}$: x_1, z_1, x_2 and z_2 components of the deflection of the center of gravity of the float caused by applied accelerations.

θ_0, θ: Direction angles of steady and vibrational accelerations from z_a axis.

$\kappa_{x1}, \kappa_{z1}, \kappa_{x2}, \kappa_{z2}$: Coefficients of compliance in x_1, z_1, x_2 and z_2 directions

$\lambda_{x2}, \lambda_{z2}$: $\lambda_{x2}=c_{x2}/M$, $\lambda_{z2}=c_{z2}/M$

φ: Phase of vibrational acceleration

$\varphi_{x2}, \varphi_{z2}$: Phase differences between the force which acts on the center of gravity G and its displacement

ϕ: Latitude of the test place (35°43′)

ω_{IA}: Input rate of gyro

ω_C: Acceleration-insensitive drift rate (Bias error)

ω_D: Total of drift rates caused by acceleration ($\omega_D=\omega_M+\omega_{a0}+\omega_a$)

ω_M: Mass unbalance drift rate

ω_{a0}, ω_a: Anisoelastic drift rates caused by steady and vibrational accelerations

f_{x2}, f_{z2}: Natural resonant frequencies depending on the gimlal deformation along x_2 and z_2 directions

3. THEORETICAL ANALYSIS

3.1 Derivation of theoretical formulae

Fig 1 shows the cross section perpendicular to the output axis of gyro. When steady acceleration α_0 acts on the gyro, the center mass of float is affected by the force $M\alpha_0$ which has parallel and opposite direction to α_0. This force and compliances κ_{x1}, κ_{z1} cause the deflection of the center of gravity from that of buoyancy, and then the torque about the output axis is generated. If we consider $|\gamma|\ll1$, x_1 and z_1 components of the force, F_{x1} and F_{z1}, and those of the deflection, δ_{x1} and δ_{z1} are as follows.

$$F_{x1}=-M\alpha_0\sin(\theta_0-\gamma)\approx-M\alpha_0\sin\theta_0 \quad (1)$$

$$F_{z1}=-M\alpha_0\cos(\theta_0-\gamma)\approx-M\alpha_0\cos\theta_0 \quad (2)$$

$$\delta_{x1}=\kappa_{x1}F_{x1} \quad (3)$$

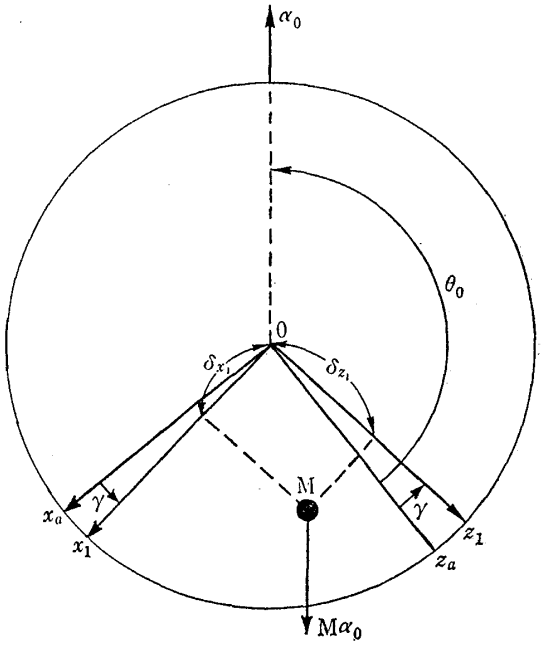

Fig. 1 Cross sectional view of gimbal

$$\delta_{z1}=\kappa_{z1}F_{z1} \quad (4)$$

The generated torque, T_{Dy1}, is as follows.

$$T_{Dy1}=\delta_{z1}F_{x1}-\delta_{x1}F_{z1} \quad (5)$$

From (1)～(5), T_{Dy1} becomes as follows.

$$T_{Dy1}=\frac{1}{2}M^2\alpha_0^2(\kappa_{z1}-\kappa_{x1})\sin 2\theta_0 \quad (6)$$

The drift rate is caused in proportion to this torque. If $\kappa_{x1}=\kappa_{z1}$, then $T_{Dy1}=0$; so that, the torque is not generated. This drift rate is called "anisoelastic error" because it is caused by the difference between κ_{x1} and κ_{z1}.

Usually steady and vibrational accelerations are simultaneously applied to the gyros mounted on a vehicle, and so we have to consider the effect of these two kinds of accelerations. Axes of compliance of the gimbal are not necessarily coincident with geometrical x_1 and z_1 axes, and there exists the damping due to the hysterisis of gimbal material and the deformation of gimbal. Based on these conditions, the elastic model of Fig 2 is determined.

We consider accelerations, compliances and damping coefficients only in the x_1z_1 plane which is perpendicular to y_1 axis, because the deflection of the center of gravity in y_1 direction is not related to the drift rate. Coefficients κ_{x2}, κ_{z2}, c_{x2} and c_{z2} vary with deflections, but those are regarded as constant because we treat a very slight deflection. Suppose steady and vibrational accelerations act on the gyro at the same time. These accelerations cause the forces which deflect the center of gravity of float. Phase of the force is different from that of accelerations. Phase difference is 180 deg with regard to the steady acceleration and is assumed to be $(180-\varphi)$ deg in the case of the vibrational one. The deflection of the center of gravity of float due to the elastic deformation of gimbal is equivalent to that of the mass M sustained by spring and dash pot according to the elastic model shown in Fig 2.

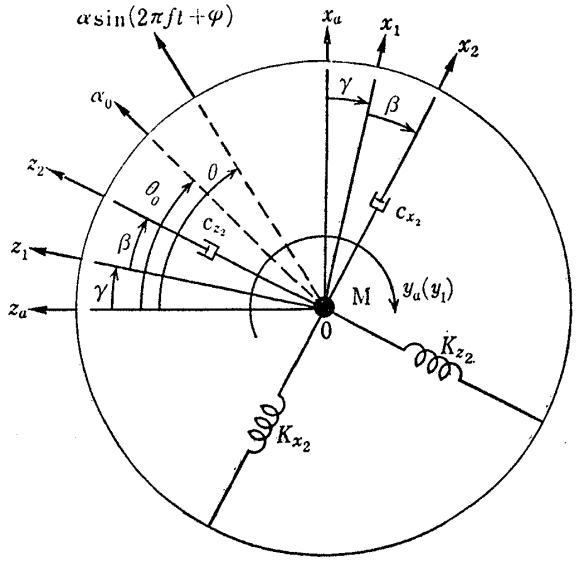

Fig. 2 Elastic model of gimbal

The force is in the direction of acceleration; however, the direction of deflection of M is generally different from that of acceleration because of the difference between two compliances. Deflections of M in x_2 and z_2 directions are proportional to the acceleration magnitude of their directions. When $\kappa_{x2}=\kappa_{z2}$ and $C_{x2}=C_{z2}$, the proportional coefficients are equal and the directions of the deflection and the force are the same. If the direction of deflection of M is different from that of the force, the torque which is equal to vector product of the deflection and the force is generated about y_1 axis. Then, its torque is equal to the vector product of the vector sum of the deflection of M and that of the force in x_2 and z_2 directions. Since the float has freedom about y_1 axis, it rotates slightly accoding to the torque, producing the drift rate.

When the direction of the deflection of M and that of the force are the same, the vector product of those is zero; then the drift rate is not caused.

Refering to Fig 2, the forces $-M\alpha_0$ and $-M\alpha\sin 2\pi ft$ act on M in the directions of steady and vibrational accelerations respectively. Considering $|\gamma|\ll 1$, we can resolve those forces in x_2 and z_2 directions.

$$F_{x2}=-M\{\alpha_0\sin(\theta_0-\beta)+\alpha\sin 2\pi ft\cdot\sin(\theta-\beta)\} \quad (7)$$

$$F_{z2}=-M\{\alpha_0\cos(\theta_0-\beta)+\alpha\sin 2\pi ft\cdot\cos(\theta-\beta)\} \quad (8)$$

The equations of motion in x_2 and z_2 directions are:

$$M\ddot{\delta}_{x2}+c_{x2}\dot{\delta}_{x2}+\delta_{x2}/\kappa_{x2}=F_{x2} \quad (9)$$

$$M\ddot{\delta}_{z2}+c_{z2}\dot{\delta}_{z2}+\delta_{z2}/\kappa_{z2}=F_{z2} \quad (10)$$

In the case of solving δ_{x2} and δ_{z2} from (7)-(10), there exist transient and steady solutions, but we neglect transient one because we consider only the deflection in steady state.

$$\delta_{x2}=-\{M\kappa_{x2}\alpha_0\sin(\theta_0-\beta)+A_{x2}(f)\alpha\sin(2\pi ft+\varphi_{x2})\sin(\theta-\beta)\} \quad (11)$$

$$\delta_{z2}=-\{M\kappa_{z2}\alpha_0\cos(\theta_0-\beta)+A_{z2}(f)\alpha\sin(2\pi ft+\varphi_{z2})\cos(\theta-\beta\} \quad (12)$$

$$A_{x2}(f)=\{4\pi^2(f^2-f^2{}_{x2})^2+\lambda^2{}_{x2}f^2\}^{-1/2}/2\pi$$

$$A_{z2}(f)=\{4\pi^2(f^2-f^2{}_{z2})^2+\lambda^2{}_{z2}f^2\}^{-1/2}/2\pi$$

$$f_{x2}=1/2\pi\sqrt{M\kappa_{x2}},\quad f_{z2}=1/2\pi\sqrt{M\kappa_{z2}}$$

$$\lambda_{x2}=c_{x2}/M,\quad \lambda_{z2}=c_{z2}/M$$

$$\tan\varphi_{x2}=\lambda_{x2}f/2\pi(f^2-f^2{}_{x2})$$

$$\tan\varphi_{z2}=\lambda_{z2}f/2\pi(f^2-f^2{}_{z2})$$

Relations between x_{1G}, y_{1G}, z_{1G} and x_{2G}, y_{2G}, z_{2G} are as follows.

$$x_{2G}=x_{1G}\cos\beta-z_{1G}\sin\beta \quad (13)$$

$$y_{2G}=y_{1G} \quad (14)$$

$$z_{2G}=x_{1G}\sin\beta+z_{1G}\cos\beta \quad (15)$$

From (7)-(15) we determine the torque T_{Dy1} about y_1 axis which is caused by steady and vibrational

accelerations.

$$\begin{aligned}T_{Dy1}&=F_{x2}(\delta_{z2}+z_{2G})-F_{z2}(\delta_{x2}+x_{2G})\\&=M\alpha_0(x_{1G}\cos\theta_0-z_{1G}\sin\theta_0)\\&\quad+M\alpha(x_{1G}\cos\theta-z_{1G}\sin\theta)\sin 2\pi ft\\&\quad+M^2\alpha_0^2(\kappa_{z2}-\kappa_{x2})\sin 2(\theta_0-\beta)/2\\&\quad+M^2\alpha\alpha_0\{\kappa_{z2}\sin(\theta-\beta)\cos(\theta_0-\beta)\\&\quad-\kappa_{x2}\cos(\theta-\beta)\sin(\theta_0-\beta)\}\sin 2\pi ft\\&\quad+M\alpha A_{z2}(f)\cos(\theta-\beta)\,[\alpha_0\sin(2\pi ft\\&\quad+\varphi_{z2})\sin(\theta_0-\beta)-\alpha\{\cos(4\pi ft+\varphi_{z2})\\&\quad-\cos\varphi_{z2}\}\sin(\theta-\beta)/2]-M\alpha A_{x2}(f)\sin(\theta\\&\quad-\beta)\,[\alpha_0\sin(2\pi ft+\varphi_{x2})\cos(\theta_0-\beta)\\&\quad-\alpha\{\cos(4\pi ft+\varphi_{x2})-\cos\varphi_{x2}\}\cos(\theta\\&\quad-\beta)/2]\end{aligned}\tag{16}$$

The equation of motion of gyro is approximately represented as follows.

$$J\ddot{\gamma}+C\dot{\gamma}+K\gamma=\omega_{IA}H+T_{Dy1}\tag{17}$$

When the disturbance torque T_{Dy1} is generated, the steady value γ_s of output angle γ is not zero even if input rate ω_{IA} is zero, and the torque $K\gamma_s$ acts on the float about output axis y_1 and the output signal is detected as drift rate ω_D, ω_D is the value of torque $K\gamma_s$ divided by angular momentum H and can be obtained when steady solution γ_s of γ is obtained by substituting zero for ω_{IA} in equations (16) and (17).

$$\begin{aligned}\omega_D&=H^{-1}K\gamma_s\\&=H^{-1}M\alpha_0(x_{1G}\cos\theta_0-z_{1G}\sin\theta_0)\,\{\alpha_0+Kq_1(f)\\&\quad\times\alpha\sin(2\pi ft+\varphi_{\gamma1})\}+H^{-1}MA_{x2}(f)\,[K\alpha q_3(f)\\&\quad\times\sin(2\pi ft+\varphi_{x2}+\varphi_{\gamma1})\sin(\theta-\beta)+0.25\alpha^2\\&\quad\times\{\cos\varphi_{x2}-Kq_2(f)\cos(4\pi ft+\varphi_{x2}+\varphi_{\gamma2})\\&\quad\times\sin 2(\theta-\beta)\}]-H^{-1}MA_{z2}(f)\,[K\alpha q_4(f)\\&\quad\times\sin(2\pi ft+\varphi_{z2}+\varphi_{\gamma1})\cos(\theta-\beta)+0.25\,\alpha^2\\&\quad\times\{\cos\phi_{z2}-Kq_2(f)\cos(4\pi ft+\varphi_{z2}+\varphi_{\gamma2})\\&\quad\times\sin 2(\theta-\beta)\}]-0.5M^2\alpha_0(\kappa_{x2}-\kappa_{z2})]\,[\alpha_0\\&\quad+Kq_1(f)\,\alpha\sin(2\pi ft+\varphi_{\gamma1})\sin 2(\theta-\beta)]\end{aligned}$$

where,

$$\begin{aligned}H^{-1}&=1/H\\q_1(f)&=\{(K-4\pi^2f^2J)^2+4\pi^2f^2C^2\}^{-1/2}\\q_2(f)&=\{(K-16\pi^2f^2J)^2+16\pi^2f^2C^2\}^{-1/2}\\q_3(f)&=4\pi^2f^2z_{2G}\{(K-4\pi^2f^2J)^2+4\pi^2f^2C^2\}^{-1/2}\\q_4(f)&=4\pi^2f^2x_{2G}\{(K-4\pi^2f^2J)^2+4\pi^2f^2C^2\}^{-1/2}\\\tan\varphi_{\gamma1}&=-\frac{2\pi fC}{K-4\pi^2f^2J}\\\tan\varphi_{\gamma2}&=\frac{K-16\pi^2f^2J}{4\pi fC}\end{aligned}$$

Thus ω_D contains vibrational terms and varies with time. But this is the solution in the case where gyro behaves according to (17) theoretically. We need determine ω_D based on the actual condition because it is not always possible that ω_D varies according to the vibrational term of T_{Dy1} and is detected. Frequency f of the vibrational acceleration which is actually applied is more than several hundreds hertzes and the gyro equipment used in this study can not respond to the torque varing with such high frequencies. Moreover, the carrier frequency in the signal detection is 400 Hz and so the amplitude modulation of the signal of frequency f higher than the carrier one is not possible. Consequently ω_D is detected according to the mean value $\overline{T}_{Dy}$ of T_{Dy1}, and also in the actual equipment ω_D is detected in this manner. The theoretical formula of drift rate is established by modifing (16) and (17) as follows.

$$\begin{aligned}\overline{T}_{Dy1}&=M\alpha_0(x_{1G}\cos\theta_0-z_{1G}\sin\theta_0)\\&\quad+M^2\alpha_0^2(\kappa_{z2}-\kappa_{x2})\sin 2(\theta_0-\beta)/2\\&\quad+M\alpha^2\{A_{z2}(f)\cos\varphi_{z2}-A_{x2}(f)\cos\varphi_{x2}\}\\&\quad\times\sin 2(\theta-\beta)/4\\&=M\alpha_0(x_{1G}\cos\theta_0-z_{1G}\sin\theta_0)\\&\quad+M^2\alpha_0^2(\kappa_{z2}-\kappa_{x2})\sin 2(\theta_0-\beta)/2\\&\quad+\frac{M\alpha^2}{4}\left\{\frac{f^2-f^2_{z2}}{4\pi^2(f^2-f^2_{z2})^2+\lambda^2_{z2}f^2}\right.\\&\quad\left.-\frac{f^2-f^2_{x2}}{4\pi^2(f^2-f^2_{x2})^2+\lambda^2_{x2}f^2}\right\}\sin 2(\theta-\beta)\end{aligned}\tag{18}$$

$$J\ddot{\gamma}+C\dot{\gamma}+K\gamma=\overline{T}_{Dy1}\tag{19}$$

From (18) and (19), the steady solution γ_0 is as follows.

$$\omega_D=K\gamma_0/H=\overline{T}_{Dy1}/H=\omega_M+\omega_{\alpha0}+\omega_\alpha\tag{20}$$

where

$$\omega_M=M\alpha_0(x_{1G}\cos\theta_0-z_{1G}\sin\theta_0)/H\tag{21}$$

$$\omega_{\alpha0}=M^2\alpha_0^2(\kappa_{z2}-\kappa_{x2})\sin 2(\theta_0-\beta)/2H\tag{22}$$

$$\omega_\alpha=\frac{M\alpha^2}{4H}\left\{\frac{f^2-f^2_{z2}}{4\pi^2(f^2-f^2_{z2})^2+\lambda^2_{z2}f^2}-\frac{f^2-f^2_{x2}}{4\pi^2(f^2-f^2_{x2})^2+\lambda^2_{x2}f^2}\right\}\sin 2(\theta-\beta)\tag{23}$$

This ω_M is derived from the deviation of the center of gravity in steady state and called "unbalanced mass drift rate", because Mx_{1G} and Mz_{1G} are unbalanced mass along input and spin axes respectively. $\omega_{\alpha0}$ and ω_α are terms due to steady and vibrational accelerations respectively, and they are independent each other. It is clear from the equations that if $\kappa_{x2}=\kappa_{z2}$ and $c_{x2}=c_{z2}$, then $f_{x2}=f_{z2}$ and $\lambda_{x2}=\lambda_{z2}$, and both $\omega_{\alpha0}$ and ω_α become zero. Both $\omega_{\alpha0}$ and ω_α are proportional to the square of the acceleration magnitude and their periods are 180° with respect to θ_0 and θ. We can forcast that ω_α varies with f and shows a remarkable frequency characteristic in the neighborhood of natural resonant frequencies f_{x2} and f_{z2} of gimbal.

3.2 Comment on theoretical formula

We consider the variation of ω_α (frequency characteristic) by substituting actual values into the equation (23) which represents the drift rate ω_α caused by the vibrational accelerations.

M=75.9 gr and H=9.931×10⁴ gr.cm²/sec are the fixed values of the experimented gyro.

The frequency characteristic of ω_α is calculated by substituting α=0.5 g, f_{x2}=1250 Hz, f_{z2}=1500 Hz,

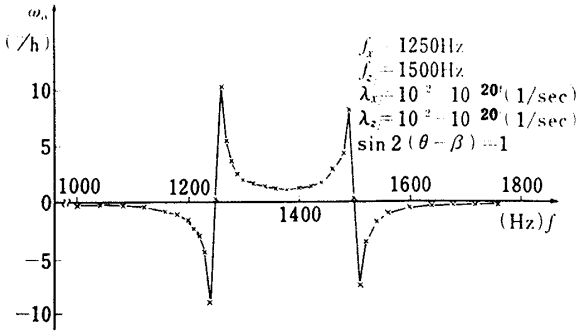

Fig. 3 Frequency characteristic of ω_α (simulation)

$\sin 2(\theta-\beta)=1$ $\lambda_{x2}=10^{-2}\sim10^{-20}$ and $\lambda_{z2}=10^{-2}\sim10^{-20}$.

The calculated value is shown in Fig 3. In this case ω_α does not vary so much according to λ_{x2} and λ_{z2} whose values are in the range of 10^{-2}–10^{-20}. For the values of λ_{x2} and λ_{z2} more than 10^{-2}, ω_α becomes smaller (even if f is in the neighborhood of f_{x2} or f_{z2}). If $\sin 2(\theta-\beta)=-1$, the sign of ω_α becomes inverse in the same frequency. ω_α is estimated to be proportional to the square of α. It is clear that ω_α grows remarkably large when the vibrational acceleration whose frequency f is in the neighborhood of f_{x2} and f_{z2} is applied. The values of f_{x2} and f_{z2} are difficult to be obtained analytically, but are estimated by the frequency characteristics of ω_α obtained from experiments. We did the simulation by a digital computer for some values of parameters f_{x2}, f_{z2}, λ_{x2} and λ_{z2}, and obtained theoretical results similar to experimental ones. We will mention those contents afterward.

4. EXPERIMENTAL ANALYSIS

In the previous chapter the tendency of drift rate is theoretically analyzed, but it should be compared with the experimental values under the action of accelerations on gyro. We measured the values of drift rates by acting steady and vibrational accelerations seperately on gyro and compared the results with theoretical analysis.

4.1 Method of the experiment

We obtained the values of drift rates caused by steady and vibrational accelerations from tumbling test and vibration experiment respectively.

The tumbling test is done by rotating the gyro at the angular rate of 200~300 deg/hour about its output axis set parallel to the polar axis of the earth. In this case input rate is zero because the gyro does not sense the earth's rotation. It is shown from Fig 4 that the gravitational acceleration which acts on the gyro in the direction perpendicular to the output axis is $g\cos\phi$, and this acceleration acts on the center of gravity of the float as steady acceleration.

In the vibration experiment the gyro is shaken horizontally by setting its output axis vertically. By this method the component of gravitational acceleration which is perpendicular to the output axis becomes zero and we can mearure the drift rate ω_D of equation (20) in which α_0 is set as zero. By regarding the output which is obtained in the non-vibrational state of the gyro ($\alpha=0$) as zero standard, the measurement is done in the state of excluding both the component of the earth's spin rate (input rate) and the drift rate independent of acceleration, and only ω_α component of ω_D can be measured. ω_α is a function of variables α, θ and f, and we can experiment for various values of these variables. The photograph shown in the page 5 is the exterior view of the shaker of the vibration test equipment used in this experiment.

4.2 Tumbling test

Action of $g\cos\phi$ on the center of gravity of the float is equivalent to accelerating the gyro case with $g\cos\phi$ and we can set $\alpha_0=g\cos\phi$ in the theoretical formula if we take θ_0 as shown in Fig 5.

The test is done by rotating the gyro clockwise about its output axis and $\theta_1(=360°-\theta_0)$ is checked instead of θ_0 for the convenince of the operation of equipment. The drift rate was measured by varying θ_1 every 5 deg from 0 to 360 deg.

Substituting $\alpha_0=g\cos\phi$, $\theta_0=360°-\theta_1$ and $\alpha=0$ into

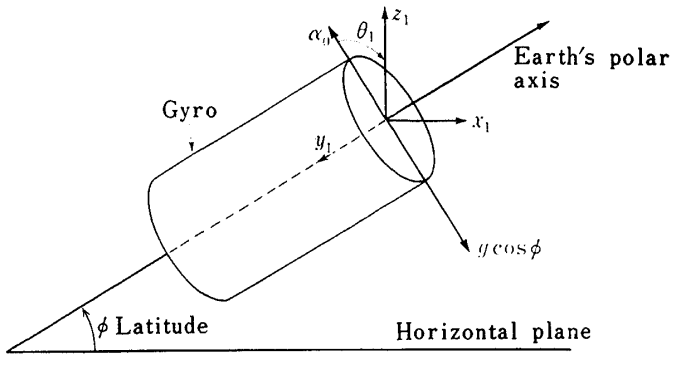

Fig. 4 Gyro output axis set parallel to earth's polar axis

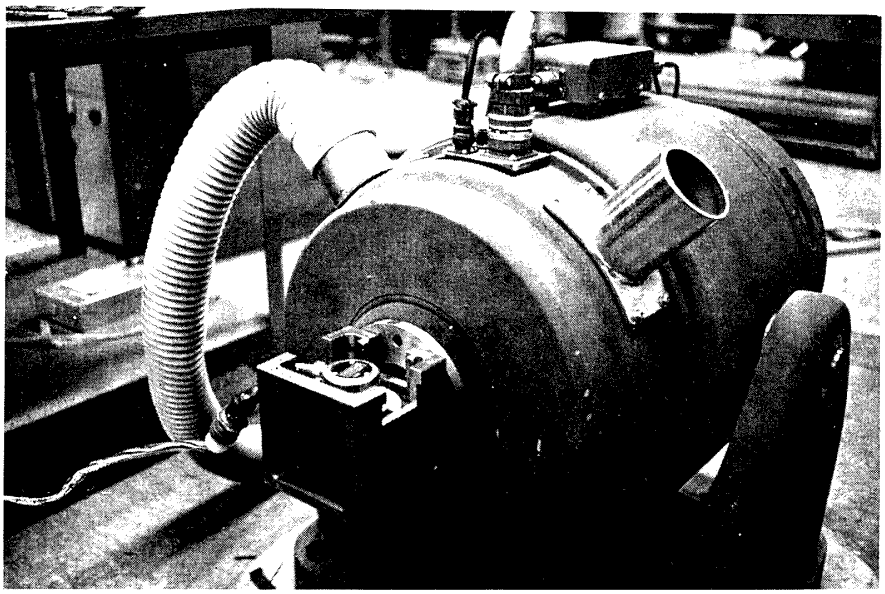

Photograph of Equipment for vibration experiment

equations (20)–(23), and including acceleration-insensitive drift rate ω_c, the total drift rate ω_{D0} under the action of steady acceleration is as follows.

$$\begin{aligned}\omega_{D0}&=\omega_c+\omega_M+\omega_{\alpha 0}\\&=\omega_c+Mg\cos\phi(x_{1G}\cos\theta_1+z_{1G}\sin\theta_1)/H\\&\quad+\{M^2g^2\cos^2\phi(\kappa_{x2}-\kappa_{z2})\sin 2\beta\}\cos 2\theta_1/2H\\&\quad+\{M^2g^2\cos^2\phi(\kappa_{x2}-\kappa_{z2})\cos 2\beta\}\sin 2\theta_1/2H\end{aligned}\qquad(24)$$

The result of tumbling test is shown in Fig 6 and Fourier analysis of Fig 6 results in the next equation.

$$\omega_{D0}=4.14-2.18\cos\theta_1+12.94\sin\theta_1+0.31\cos 2\theta_1-1.06\sin 2\theta_1(^\circ/\mathrm{h})\qquad(25)$$

By substituting the values of M, g, ϕ and H which are shown in the nomenclature into equation (24), ω_c, x_{1G}, z_{1G} and β are obtained from equations (24) and (25).

$$\omega_c=4.14^\circ/\mathrm{h}$$

$$x_{1G}=-0.174\times10^{-4}\,\mathrm{cm},\quad z_{1G}=0.116\times10^{-3}\,\mathrm{cm}$$

$$\beta=-8\mathrm{deg}$$

The anisoelastic error caused by steady acceleration is usually expressed as the value of the coefficient of second harmonic wave in equation (25) divided by $\cos^2\phi$ so that the value can be normalized under the action of 1 g acceleration and the value is $1.7^\circ/\mathrm{h/g^2}$ in this case.

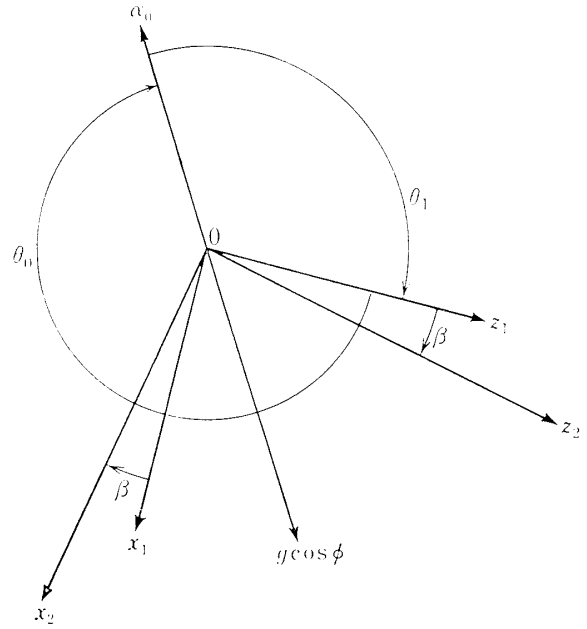

Fig. 5 Plane figure of gyro seen from the polar star

4.3 Vibration experiment

Vibration experiment 1

Frequency f must be a proper constant value in order to measure ω_α corresponding to the variation of α and θ. We chose 580 Hz as f, because the vibration wave form of the shaker was not deformed in this frequency. Fixing $f=580$ Hz, θ was varied

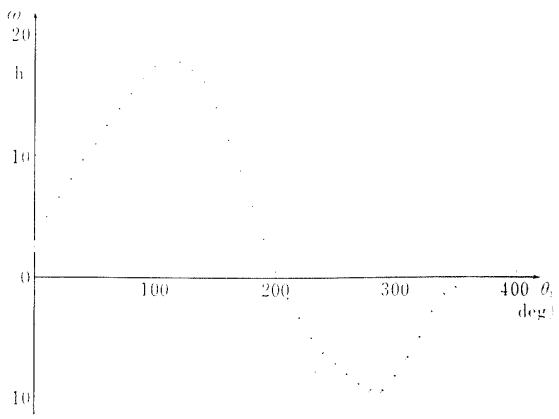

Fig. 6 Result of tumbling test

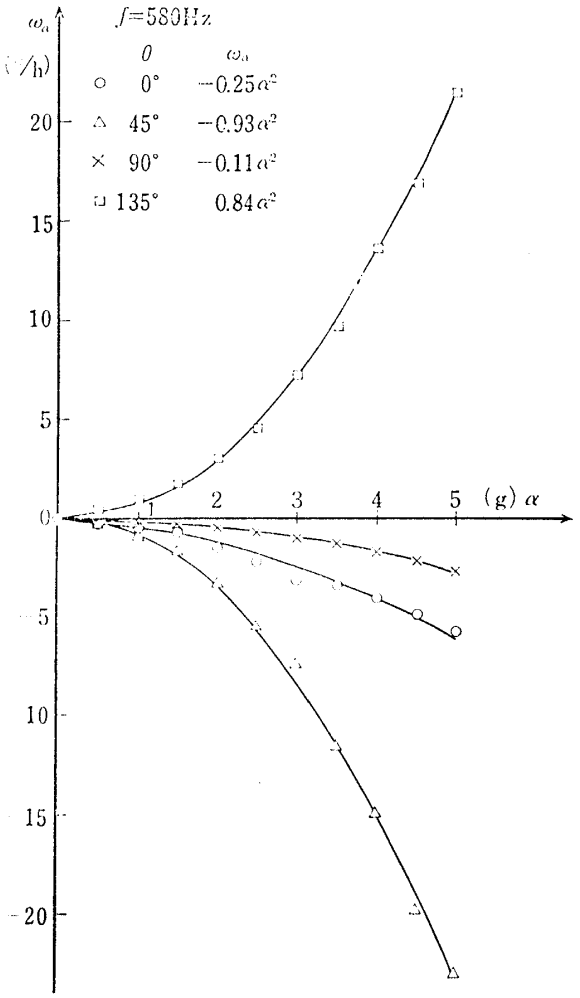

Fig. 7 Relations between ω_α and α

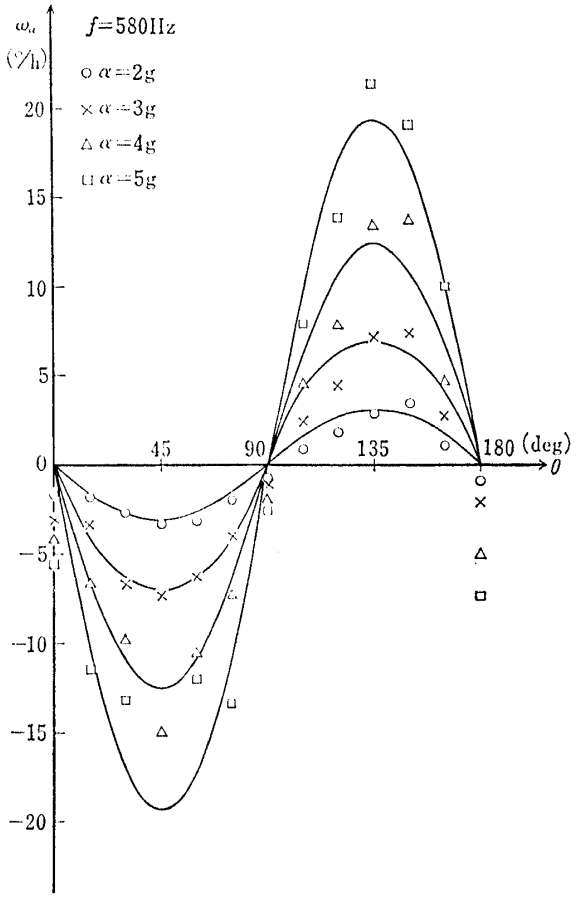

Fig. 8 Relations between ω_α and θ

every 15 deg from 0 to 180 deg, and in each θ ω_α was measured at the increment of 0.5 g of α from 0 to 5 g.

Fig 7 shows one example of the experimental values of ω_α corresponding to α for several values of θ. It is clear from equation (23) that ω_α is proportional to α^2 and the quadratic curves which are obtained from the experimental values by the method of least squares are shown in Fig 7.

Fig 8 shows ω_α versus θ in the same experimental values as Fig 7, where α is a parameter. ω_α is proportional to $\sin 2(\theta-\beta)$. The curves of Fig 8 show the fundamental waves (the term proportional to $\sin 2(\theta-\beta)$ and obtained from the exprimental values by Fourier analysis).

Vibration experiment 2

The gyro was experimented under the vibrational accelerations whose frequency f was swept in the range of 100 to 3000 Hz in θ=0°, 45° and 135° holding α constant (=0.5 g). Fig 9~11 show the experimental results of ω_α for f. It is found from the obtained values that the remarkable variation of frequency characteristic appears in the domain of 900 to 1700 Hz. The sign of ω_α in the case of θ=135° is the inverse of one in the case of θ=45° because the period of ω_α is 180° with respect to θ in the same frequency. The value of α should not be increased because the gimbal will be destroyed for larger value of α, but we could obtain the dis-

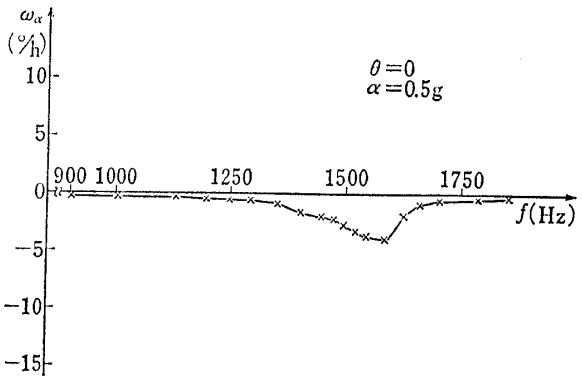

Fig. 9 Frequency characteristic of ω_α (Experimental result)

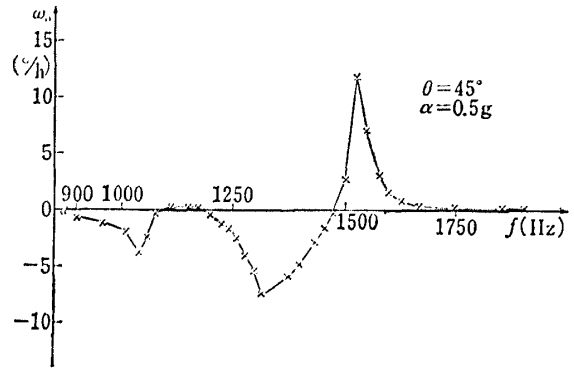

Fig. 10 Frequency characteristic of ω_α (Experimental result)

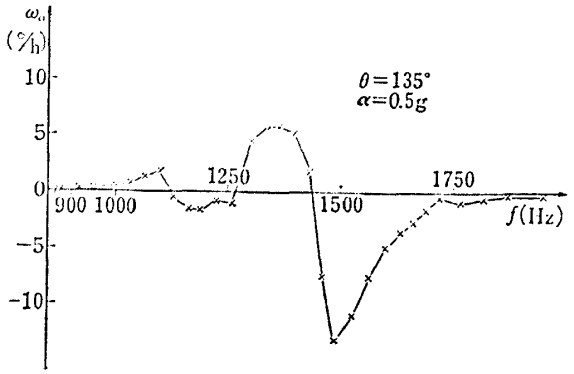

Fig. 11 Frequency characteristic of ω_α (Experimental result)

tinct frequency characteristics for α=0.5 g.

5. CONSIDERATIONS

It is examined how the results of vibration experiments done according to each variable of the theoretical formula are similar to the theory.

5.1 Considerations on the vibration experiment 1

Characteristic of ω_α which is proportional to α^2 is in accordance with the theoretical formula because the experimental results in Fig 7 show the tendency of quadratic curve concerning α. Positive and negative values of ω_α with respect to θ are foreseen from the proportional characteristic to $\sin 2(\theta-\beta)$. Experimental values of ω_α vary in proportion to $\sin 2(\theta-\beta)$ as seen in Fig 8.

5.2 Considerations on the vibration experiment 2

Theoretical analysis shows that the value of ω_α grows remarkably in frequency f near f_{x2} and f_{z2}, and we compare theory with experimental results about various parameters f_{x2}, f_{z2}, λ_{x2} and λ_{z2}. Fig 12~15 show simulation results of frequency characteristics of ω_α in the parameters shown in table 1.

The values of α, M and H used in the experiments are used in this simulation. Magnitude and sign of ω_α varies with $\sin 2(\theta-\beta)$.

The values of ω_α grow remarkably at the frequencies near f_{x2} and f_{z2}, and also vary with λ_{x2} and λ_{z2}.

If we choose the values of λ_{x2} and λ_{z2} as the calculated values of ω_α consist with the experimental

Table 1. Parameter values in simulation

	Fig 12	Fig 13	Fig 14	Fig 15	Uuit
f_{x2}	750	1,000	1,250	1,750	Hz
f_{z2}	1,500	1,500	1,500	1,500	Hz
λ_{x2}	$10^{2.6}$	$10^{2.6}$	$10^{2.6}$	$10^{2.4}$	1/sec
λ_{z2}	10^{-1}~10^{-20}	10^{-1}~10^{-20}	10^{-1}~10^{-20}	10^{-1}~10^{-20}	1/sec
$\sin 2(\theta-\beta)$	1	1	1	1	1

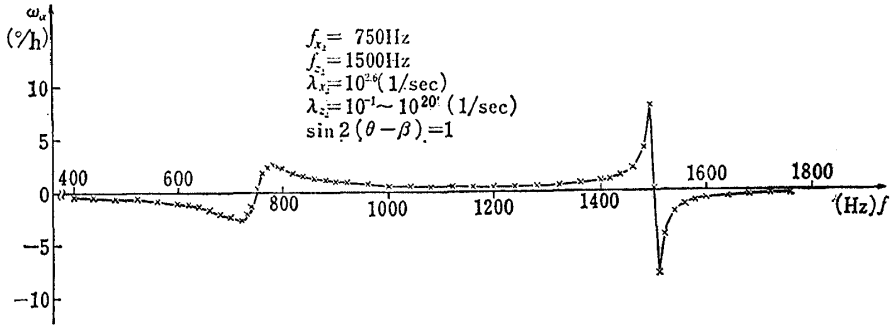

Fig. 12 Frequency characteristic of ω_α (simulation)

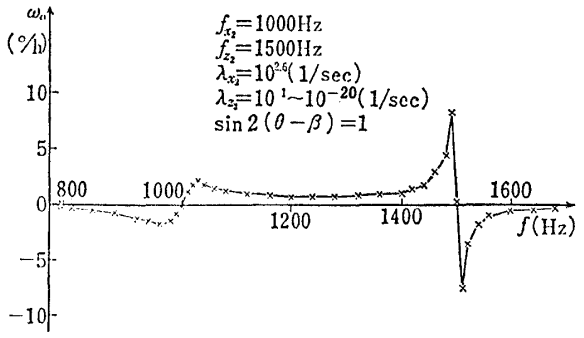

Fig. 13 Frequency characteristic of ω_α (simulation)

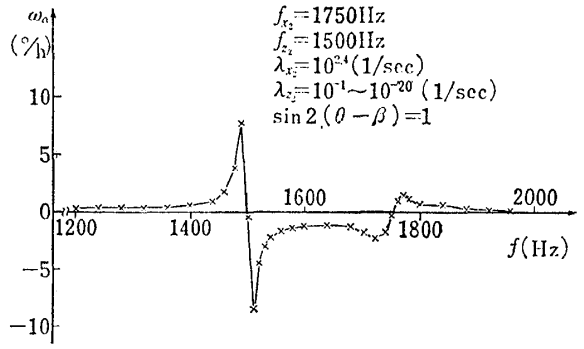

Fig. 14 Frequency characteristic of ω_α (simulation)

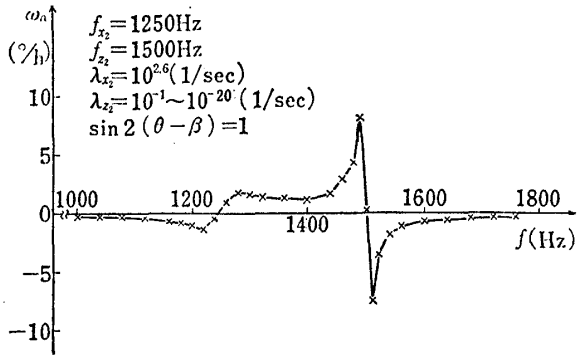

Fig. 15 Frequency characteristic of ω_α (simulation)

values all over the frequency, λ_{x2} and λ_{z2} become $10^{2.6}$ and $10^{-1}\sim10^{-20}$ respectively. Because f_{x2}, λ_{x2} and f_{z2}, λ_{z2} are shown seperately in the formula of ω_α, if we exchange them, sign of ω_α becomes inverse. When we exchange the value of f_{x2} for that of f_{z2}, the values of ω_α show the exchanged magnitude at f near f_{x2} and f_{z2}.

The theoretical formulae were derived by regarding each parameter as constant and theoretically calculated values (simulation result) show more remarkable frequency characteristics in comparison with the experimental results near the resonant frequencies. However, as those show similar tendency, it is clear that frequnecy characteristics obtained from experiments show natural resonance of the gimlal as predicted in theory.

5.3 Evaluation of Gyro errors

We usually represent the magnitude of anisoelastic errors in the vibration experiment by the value obtained in the state of acceleration with frequency less than 1000 Hz and the magnitude of 1 g r.m.s (root mean square) where there does not exist natural rosonance. In this study resonant frequency is higher than 1000 Hz and maximum absolute value of ω_α which we obtained is 1.7°/h/g²rms in the state where the frequency of vibrational acceleration f is 580 Hz. This value is very similar to the rusult of the tumbling test and so it is clarified that the gyro anisoelastic error can be generally evaluated only by tumbling test. The anisoelastic errors of the gyro used in this study are very large, but it is our aim in the development of recent gyros to decrease their values in less than $0.1°/h/g^2$, and it will be possible to realize such a small value.

6. CONCLUSION

Theoretical formulae and experimental results show similar tendencies with respect to the magnitude and the directions of vibrational accelerations, and with respect to the frequency characteristics.

Therefore, the theoretical treatment is appropriate about gyro errors caused by deflection of the center of gravity (under the action of acceleration) according to elastic model of Fig 2 and we could clarify the characteristic of anisoelastic errors by vibrational accelerations. It is necessary to decrease the anisoelastic effect of the gimbal system containing spin rotor bearings for improving the accuracy of a gyro.

We acknowledge Mr. Kazuo Higuchi, the head of Instrumentation and Control Devision of National Aerospace Laboratory who gave us proper guidance to promote this study.

References

1) G.R. Mocomber and M. Fernandez; Inertial Guidance Engineering, Prentice Hall Inc. (1962) (pp. 492–496)
2) C.S. Draper, W. Wrigly and J. Hovorka; Inertial Guidance, Pergamon Press Inc. (1960) Chapt. 7)
3) G.A. Slomyanskiy; Determining Maximum Values of Gravitational Drift and Drift from Unequal Rigidity of Floating Integration Gyroscopes, Moscow Aviatsionnyy Tekhnologicheskiy Institut Trudy, No. 59, 1964 (pp. 74–82)
4) G.E. Pitman; Inertial Guidance, Universty of California Engineering and Physical Sciences Extension series (1962) (pp. 79–84)

5) 森 大吉郎; 観測ロケットの機体の振動特性について, 航空学会誌第7巻64号
6) C.M. Harris & C.E. Crede; Shock and Vibration Handbook, vol 3, 47 (Shock and vibration aircraft and missiles)

APPENDIX

A SINGLE-DEGREE-OF-FREEDOM GYRO

1. Nomenclature

We derive the equation of motion of a single-degree-of-freedom gyro considering the motion of rotor, gimbal and vehicle respectively. Gyro case is rigidly fixed in a vehicle, the center of rotor and that of gimbal are coincident at the point 0, and the rotor is rotationally symmetric about its spin axis.

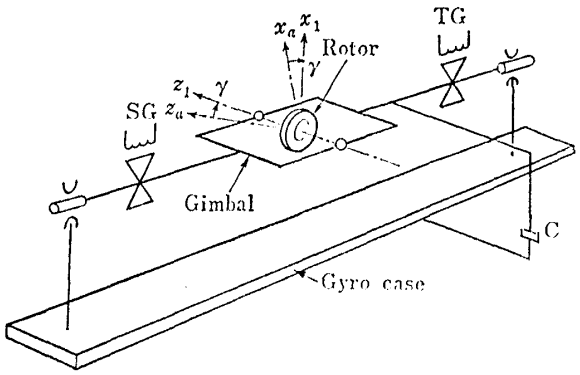

Fig. A

$\boldsymbol{H}_0$	Angular momentum vector of rotor
$\boldsymbol{H}_1$	Angular momentum vector of gimbal
$\boldsymbol{H}$	Total angular momentum vector of float ($\boldsymbol{H}=\boldsymbol{H}_0+\boldsymbol{H}_1$)
$H_{0z1}(=H)$	Component of $\boldsymbol{H}_0$ along spin axis ($H_{0z1}=I_{0z1}n$)
$\boldsymbol{i}_a, \boldsymbol{j}_a, \boldsymbol{k}_a$	Unit vectors along x_a, y_a and z_a axes
$\boldsymbol{i}_1, \boldsymbol{j}_1, \boldsymbol{k}_1$	Unit vectors along x_1, y_1 and z_1 axes
$I_{0x1}, I_{0y1}, I_{0z1}$	Moments of inertia of rotor about x_1, y_1 and z_1 axes
$I_{1x1}, I_{1y1}, I_{1z1}$	Moments of inertia of gimbal about x_1, y_1 and z_1 axes
$I_x, I_y(=J)$	Moments of inertia of float about x_1 and y_1 axes $I_{x1}=I_{0x1}+I_{1x1}$, $I_{y1}=I_{0y1}+I_{1y1}$
I_G	Output current
K	Spring constant of gyro control system (Elastic restraint constant)
K_{SG}	Sensitivity of signal generator
K_A	Amp gain
K_{TG}	Sensitivity of torque generator
n	Spin velocity of rotor and $n=\omega_{0z1}$
0–$x_a y_a z_a$	Case-fixed coordinate system (that is, Vehiche-fixed coordinate system)
0–$x_1 y_1 z_1$	Gimbal-fixed coordinate system
$0_{x1}, 0_{y1}, 0_{z1}$	Input, output and spin axes
$\boldsymbol{T}_d$	Driving torque given to the rotar by gimbal for rotation
$\boldsymbol{T}_1$	Torque caused by the drag of rotor to gimbal
$\boldsymbol{T}_f$	Frictional resistance torque between rotor and gimbal
$\boldsymbol{T}_a$	Torque given to the float by the vehicle
$\boldsymbol{T}_D$	Disturbance torque acting on the float
T_{dz1}, T_{fz1}	z_1 components of $\boldsymbol{T}_d$ and $\boldsymbol{T}_f$
$T_{ax1}, T_{ay1}, T_{az1}$	x_1, y_1 and z_1 components of $\boldsymbol{T}_a$
$T_{Dx1}, T_{Dy1}, T_{Dz1}$	x_1, y_1 and z_1 components of $\boldsymbol{T}_D$
$\boldsymbol{T}_c$	Damping torque between float and case (Element of $\boldsymbol{T}_{ay1}$)
$\boldsymbol{T}_G$	Torque given to the float by torque generator (Element of $\boldsymbol{T}_{ay1}$)
γ	Output angle of gyro
$\boldsymbol{\omega}_0, \boldsymbol{\omega}_1, \boldsymbol{\omega}_a$	Angular velocity vectors of rotor, gimbal and vehicle to the inertial space
$\omega_{0x1}, \omega_{0y1}, \omega_{0z1}$	x_1, y_1 and z_1 components of $\boldsymbol{\omega}_0$
$\omega_{1x1}, \omega_{1y1}, \omega_{1z1}$	x_1, y_1 and z_1 components of $\boldsymbol{\omega}_1$
$\omega_{ax1}, \omega_{ay1}, \omega_{az1}$	x_1, y_1 and z_1 components of $\boldsymbol{\omega}_a$
$\omega_{axa}, \omega_{aya}, \omega_{aza}$	x_a, y_a and z_a components of $\boldsymbol{\omega}_a$
ω_{IA}	Input rate of gyro ($\omega_{IA}=\omega_{ax1}=\omega_{1x1}$)

2. Equation of motion

We resolve angular velocities $\boldsymbol{\omega}_0$, $\boldsymbol{\omega}_1$, $\boldsymbol{\omega}_a$ into components respectively.

$$\boldsymbol{\omega}_0=\omega_{0x1}\boldsymbol{i}_1+\omega_{0y1}\boldsymbol{j}_1+\omega_{0z1}\boldsymbol{k}_1 \quad (1)$$

$$\boldsymbol{\omega}_1=\omega_{1x1}\boldsymbol{i}_1+\omega_{1y1}\boldsymbol{j}_1+\omega_{1z1}\boldsymbol{k}_1 \quad (2)$$

$$\boldsymbol{\omega}_a=\omega_{axa}\boldsymbol{i}_a+\omega_{aya}\boldsymbol{j}_a+\omega_{aza}\boldsymbol{k}_a=\omega_{ax1}\boldsymbol{i}_1+\omega_{ay1}\boldsymbol{j}_1+\omega_{az1}\boldsymbol{k}_1 \quad (3)$$

By relations of degree of freedom

$$\omega_{0x1}=\omega_{1x1}=\omega_{ax1},\ \omega_{0y1}=\omega_{1y1} \quad (4)$$

ω_{0z1} is the spin velocity of rotor, and

$$\omega_{0z1}=n \quad (5)$$

If we express ω_{1x1}, ω_{1y1} and ω_{1z1} by using components of $\boldsymbol{\omega}_a$ and γ,

$$\omega_{1z1}=\omega_{axa}\cos\gamma-\omega_{aza}\sin\gamma \quad (6)$$

$$\omega_{1y1}=\omega_{ay1}+\dot{\gamma}=\omega_{aya}+\dot{\gamma} \quad (7)$$

$$\omega_{1z1}=\omega_{axa}\sin\gamma+\omega_{aza}\cos\gamma \quad (8)$$

$\boldsymbol{H}_0$ and $\boldsymbol{H}_1$ are angular momenta of rotor and gimbal respectively,

$$\boldsymbol{H}_0=I_{0x1}\omega_{0x1}\boldsymbol{i}_1+I_{0y1}\omega_{0y1}\boldsymbol{j}_1+I_{0z1}\omega_{0z1}\boldsymbol{k}_1=I_{0x1}\omega_{1x1}\boldsymbol{i}_1+I_{0y1}\omega_{1y1}\boldsymbol{j}_1+I_{0z1}n\boldsymbol{k}_1 \quad (9)$$

$$\boldsymbol{H}_1=I_{1x1}\omega_{1x1}\boldsymbol{i}_1+I_{1y1}\omega_{1y1}\boldsymbol{j}_1+I_{1z1}\omega_{1z1}\boldsymbol{k}_1 \quad (10)$$

$$\boldsymbol{H}=\boldsymbol{H}_0+\boldsymbol{H}_1=I_{x1}\omega_{1x1}\boldsymbol{i}_1+I_{y1}\omega_{1y1}\boldsymbol{j}_1+(H_{0z1}+I_{1z1}\omega_{1z1})\boldsymbol{k}_1 \quad (11)$$

As the rotor is rotational body

$$I_{0x1}=I_{0y1} \quad (12)$$

The time variations of $\boldsymbol{H}_0$ and $\boldsymbol{H}_1$ are as follows.

$$\dot{\boldsymbol{H}}_0=(\dot{\boldsymbol{H}}_0)_1+\boldsymbol{\omega}_1\times\boldsymbol{H}_0=\boldsymbol{T}_1+\boldsymbol{T}_d+\boldsymbol{T}_f \quad (13)$$

$$\dot{\boldsymbol{H}}_1=(\dot{\boldsymbol{H}}_1)_1+\boldsymbol{\omega}_1\times\boldsymbol{H}_1=-\boldsymbol{T}_1+\boldsymbol{T}_a \quad (14)$$

Rotor and gimbal are influenced by disturbance torques derived from air flow and deflection of the center of gravity. Of course, the assumption in deriving the equation of motion cannot be realized if the center of gravity deflects, but we need not consider the angular momentum and its variation because its deflection is very small. However, the torque caused by above-mentioned defletion is generally large, and so we need add its torque to the equation of motion.

When n is constant,

$$\dot{n}=0,\ \boldsymbol{T}_d+\boldsymbol{T}_f=(Td_{z1}+T_{fz1})=0 \quad (15)$$

From (9)-(15), we set the the equation of motion by resolving into each component and add the component of T_D.

$$I_{x1}\dot{\omega}_{1x1}+H_{0z1}\omega_{1y1}-(I_{y1}-I_{1z1})\omega_{1y1}\omega_{1z1}=T_{ax1}+T_{Dx1} \quad (16)$$

$$I_{y1}\dot{\omega}_{1y1}-H_{0z1}\omega_{1x1}+(I_{x1}-I_{1z1})\omega_{1z1}\omega_{1x1}=T_{ay1}+T_{Dy1} \quad (17)$$

$$I_{1z1}\dot{\omega}_{1z1}+(I_{1y1}-I_{1x1})\omega_{1x1}\omega_{1y1}=T_{az1}+T_{Dz1} \quad (18)$$

By using (6), (7) and (8), equations (16), (17) and (18) are expressed as follows.

$$I_{x1}(\dot{\omega}_{axa}\cos\gamma-\dot{\omega}_{aza}\sin\gamma)+\{H_{0z1}-(I_{y1}-I_{1z1})\times(\omega_{axa}\sin\gamma+\omega_{aza}\cos\gamma)\}\omega_{aya}+\{H_{0z1}-(I_{1x1}+I_{1y1}-I_{1z1})(\omega_{axa}\sin\gamma+\omega_{aza}\cos\gamma)\}\dot{\gamma}=T_{ax1}+T_{Dx1} \quad (19)$$

$$I_y(\dot{\gamma}+\dot{\omega}_{aya})+\{-H_{0z1}+(I_{x1}-I_{1z1})(\omega_{axa}\sin\gamma+\omega_{aza}\cos\gamma)\}(\omega_{axa}\cos\gamma-\omega_{aza}\sin\gamma)=T_{ay1}+T_{Dy1} \quad (20)$$

$$I_{1z1}(\dot{\omega}_{axa}\sin\gamma+\dot{\omega}_{aza}\cos\gamma)+(I_{1y1}-I_{1x1})\times(\omega_{axa}\cos\gamma-\omega_{aza}\sin\gamma)\omega_{aya}+(I_{1z1}+I_{1y1}-I_{1x1})(\omega_{axa}\cos\gamma-\omega_{aza}\sin\gamma)\dot{\gamma}=T_{az1}+T_{Dz1} \quad (21)$$

3. Gyro equipment

We apply the equation of motion to the gyro used in this study (a floated single-degree-of-freedom gyro). This gyro, whose input rate is ω_{ax1}, is devised so that ω_{IA} is obtained by measuring output angle γ. Among (19), (20) and (21), the equation (20) is important in getting ω_{ax1} by applying them to the gyro equipment. Adapting to the practical state we derive the approximate equation of (20) under the following assumption.

$$\omega_{aya}=\text{const} \quad (22)$$

$$H_{0z1}\gg(I_{x1}-I_{1z1})(\omega_{axa}\sin\gamma+\omega_{aza}\cos\gamma) \quad (23)$$

From (20), (22) and (23)

$$I_{y1}\ddot{\gamma}-H_{0z1}(\omega_{axa}\cos\gamma-\omega_{aza}\sin\gamma)=T_{ay1}+T_{Dy1} \quad (24)$$

Bearing friction between gimbal and case is generally unavoidable in the gyro. In order to reduce this friction and stabilize the output indication we use the method how the gimbal in which the rotor is hermetically contained is floated in the viscous oil. This kind of gyro is called a floated single-degree-of-freedom gyro and the gimbal (with rotor) is called float. The float rotates at the angular velocity $\dot{\gamma}$ about y_1 axis and is given torque T_c proportional to $-\dot{\gamma}$ by the frictional resistance to the oil.

Output angle γ is converted into electric voltage in S.G. (signal generator) and becomes output current I_G in T.G (torque generator) after being amplified by the amplifier. T.G generates torque T_G proportional to $-I_G$ and gives it to the float. If each characteristic of S.G, Amp and T.G is linear, T_G is proportional to $-\gamma$. As T_C and T_G become the component (T_{ay1}) along y_1 axis of the torque $\boldsymbol{T}_a$ which is given to the float by a vehicle,

$$T_{ay1}=T_C+T_G=-(C\dot{\gamma}+K\gamma) \quad (25)$$

$$K=K_{SG}K_AK_{TG} \quad (26)$$

From (24), (25), (26)

$$I_{y1}\ddot{\gamma}+C\dot{\gamma}+K\gamma=H_{0z1}(\omega_{axa}\cos\gamma-\omega_{aza}\sin\gamma)+T_{Dy1} \quad (27)$$

From (4), (6), (27)

$$J\ddot{\gamma}+C\dot{\gamma}+K\gamma=H\omega_{ax1}+T_{Dy1}=\omega_{IA}H+T_{Dy1} \quad (28)$$

ω_{IA} is described as $\omega_{IA}=\omega_{ax1}=\omega_{axa}\cos\gamma-\omega_{aza}\sin\gamma$ but γ is very small ($|\gamma|\ll1$) in the practical equipment. Freedom of γ is ±3 deg in the gyro used in this study and we can effectively use γ in the range of maximum value ±0.1 deg in practice. Accordingly we can regard $\sin\gamma$ as zero and $\cos\gamma$ as 1 and take approximate equation $\omega_{IA}=\omega_{1x1}=\omega_{ax1}=\omega_{axa}$.

If $T_{Dy}=0$, the equation $\omega_{IA}=K_{TG}\cdot I_G/H$ is stationally realized and ω_{IA} can be known because H and K_{TG} are foreseen in the gyro. If $T_{Dy1}\neq0$, we cannot know input rate ω_{IA} through I_G, but can know the input rate which containes error. This error is called, "drift rate".

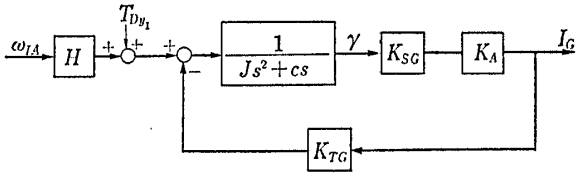

Fig. B

TR-183	Experimental Investigation of Strength of Axial Flow Compressor Blade Root —Pin Joints Lug having Clearance between Pin and Pin Hole—	Tameji IKEDA & Takashi YAMAGISHI	Sep. 1969
TR-184-T	An Improved Method of Designing and Calculating the Minimal Wave Drag Configuration by Supersonic and Moment-of-Area Rules	Kenneth K. YOSHIKAWA	Oct. 1969
TR-185	Thermal Characteristics of FPR Rocket Nosecone	Koichi OGAWA & Shuji ENDO	Nov. 1969
TR-186	The Analysis on Transmission-Line Rocket Antennas	Jyoji TABATA, Yoshio SAKURAI, Masao MIURA, Yoshitsugu MATSUZAKI & Norio TSUKAMOTO	Dec. 1969
TR-187	A Magnetic Attitude Measuring Instrument Applying the Holl Effect	Shigeru KIMURA, Jyoji TABATA & Yoshitsugu MATSUZAKI	Dec. 1969

TECHNICAL REPORT OF NATIONAL AEROSPACE LABORATORY
TR-188T

航空宇宙技術研究所報告 188T 号 (欧文)

昭和 48 年 6 月 発行

発行所 航空宇宙技術研究所
東京都調布市深大寺町 1,880
電話 武蔵野三鷹 (0422)47-5911 (大代表)

印刷所 株式会社 東京プレス
東京都板橋区桜川 2 丁目 27 の 12

Published by
NATIONAL AEROSPACE LABORATORY
1,880 Jindaiji, Chōfu, Tokyo
JAPAN

Printed in Japan